Applied Numerical Mathematics 59 (2009) 1989–2001

Contents lists available at ScienceDirect

Applied Numerical Mathematics

www.elsevier.com/locate/apnum

Computational and conditioning issues of a discrete model for cochlear sensorineural hypoacusia ☆

Daniele Bertaccini *, Stefano Fanelli

Università di Roma "Tor Vergata", viale della Ricerca Scientifica, 00133 Roma, Italy

A R T I C L E   I N F O

Article history:
Received 10 January 2008
Received in revised form 19 February 2009
Accepted 10 March 2009
Available online 18 March 2009

Keywords:
Cochlear modeling
Iterative methods
Integrodifferential models
Conditioning

A B S T R A C T

The interest of inner ear research towards the cochlear simulation is due to the lack of imaging techniques for human noninvasive investigation. Unfortunately, in case of Sensorineural Hearing Loss (SHL), the majority of the models developed in the literature do not take into consideration all the complex audiological phenomena occurring in the Organ of Corti. In this paper we show that a realistic analysis of recruitment and hyperacusis can be effectively reproduced by nonlinear modeling. The latter fact is in contrast to the classical assumption that an impaired ear with a moderate SHL can be effectively described by a passive linear model. In order to deal with the active role performed by the Outer Hair Cells (OHC), recent models based on integro-differential equations were introduced in the literature. However, the discretization and the computational methods present some issues. In this work we suggest the utilization of a variable-step-variable order package to advance in time in order to preserve the character of the continuous solution. Moreover, we illustrate that, in case of SHL, the fixed-point approach for the linear algebraic system generated by the discretization can be inappropriate. Since preliminary experiences show that the matrices involved in the model present clustered eigenvalues, we propose Krylov methods. Numerical tests are included in order to confirm the effectiveness of the proposal.

1. Introduction

Cochlear modeling represents an important research tool in the study of inner ear disease and pathology. In the last decades several mathematical models were introduced in the literature with the main aim of investigating the microscopic details of this "inaccessible" structure of the sensorineural part of the auditive system (see, f.i. [3,5–7]). In particular, a three-dimensional model was described in [12] in order to obtain a realistic simulation of the complex processes taking place in the Organ of Corti. More recently, a remarkable and operational two-dimensional model was introduced in [10], by coupling the classical second order linear Partial Differential Equations (PDE) for the Basilar Membrane (BM) with a nonlinear active and discrete feed-forward Outer Hair Cells (OHC) model.

We emphasize that the complete model is based on a system of integro-differential equations presenting many difficulties from a numerical point of view. The discretization scheme and the corresponding algorithm utilized in [10] is certainly extremely interesting, but, unfortunately, has some disadvantages.

Firstly, the discretized systems strongly depend on the expansion of some truncated series. Secondly, the time step Δt should be chosen small enough in order to achieve the convergence of the fixed point iteration algorithm, thereby implying a possible waste of computational resources. A more efficient procedure can be implemented by a numerical approach with

☆ Revised version date: February 11, 2009. This work is partially supported by MIUR, grant 2006017542 and by NIH grant GM 66309-01.
* Corresponding author.
E-mail addresses: bertaccini@mat.uniroma2.it (D. Bertaccini), fanelli@mat.uniroma2.it (S. Fanelli).

0168-9274/$30.00
doi:10.1016/j.apnum.2009.03.001

adaptive meshes in time using *projective iterative methods* to solve the discrete problem at each step and, therefore, with a potentially more robust strategy.

Moreover, it must be stressed that, due to anatomical reasons, the processing of the auditive signals is a *discrete system*, since it takes place in the tonotopic sites of the cochlea. Modeling the Organ of Corti with continuous integro-differential equations is quite useful from a mathematical point of view, but it is, in fact, a stylization of the reality. Hence, the discrete approximation associated to the numerical solution has to take into account this fundamental anatomical feature.

It is also important to point out that the paper [10] was mainly oriented to the modeling of patients with normal hearing or, more precisely, *without a Sensorineural Hearing Loss* (SHL). The convergence of the corresponding numerical method was in fact guaranteed by assuming that the gain factor $\alpha(x,u)$ of the active part of the model could be efficiently described by an integral function of the BM displacement $u(x,t)$ and $\max_u\{\alpha(x,u)\}$ be everywhere less than one with a suitably small time step.

In [11] the model was extended to the case of patients with several levels of SHL in order to investigate the possible medical applications. As a matter of fact, the principal goal of the latter paper was to enhance the ability of impaired hearing by a sound amplification method, which is a fundamental problem in the optimization of the digital performances of the last generation hearing aids.

The main difficulty of a realistic modeling of the impairment due to a SHL with a damage limited to OHC is the correct simulation of a phenomenon called *recruitment* and the consequent *hyperacusis*. Patients with intact Inner Hair Cells (IHC) and a complete loss of OHC show in fact a deafness characterized by a SHL of 50–60 decibel or, for short, dB, a dramatic deficit of frequency discrimination and a painful hyperacusis above a sound level of 80–90 dB, particularly in the high frequencies (see [14,15]).

Thus, a strong reduction of the dynamical auditive range is one of the most important consequences of SHL. From a mathematical point of view, this type of SHL can be effectively reproduced only by suitable nonlinear modeling. Therefore, the fact that *an impaired ear with a damage limited to the* OHC *has a complete lack of the compressive nonlinearity of a normal ear does not correspond to the reality and the auditive behavior in the latter case cannot be described by a linear passive model*.

Hyperacusis, in particular, plays a crucial role in SHL and represents a critical constraint in the adaptive gain strategy of the hearing aids. Audiological experience shows that many patients with steep slope audiograms cannot obtain a real benefit from hearing aids, in contrast to the theoretical amplification curves computed by the digital models implemented in the acoustic laboratories [9].

In this paper we have tried to modify the model described in [11], by introducing a gain factor $\hat{\alpha}$ that should be able to reproduce the auditive phenomena of an impaired ear with a loss limited to the OHC. We underline that this type of SHL is the most frequent one, since it is typical of presbyacusis, noise damage or acoustic trauma [14].

From a numerical point of view it is important to notice that recruitment and hyperacusis can be seen as a sort of numerical ill-conditioning of the integro-differential equations. More precisely, in this work we show that the matrices involved in the computational scheme can be ill-conditioned since our new gain factor $\hat{\alpha}$ can now assume values greater than one. Due to the cited *intrinsic discrete nature* of OHC processing, this numeric interpretation of recruitment and hyperacusis seems to be promising and deserves further investigation.

2. From the continuous to the discrete model

An advanced operational model for the Organ of Corti couples classical linear partial differential equations for the Basilar Membrane (BM) (i.e. the mathematical translation of classical Von Bèkèsy's model [17]) with nonlinear and nonlocal integro-differential equations for the OHC, thereby properly describing the active role of these fundamental cells.

Firstly, we summarize the model introduced in [10].

In the latter model the forces applied by OHC on the BM are assumed proportional to the total force acting on the BM (OHC act like piezo-electric actuators that push BM). The force applied on the BM is transmitted to the OHC, which act on the cilia and back on the BM.

Let $p(x,0,t)$ and $F_{\text{cell}}(x,t)$ be the pressure across the BM and the force transmitted by OHC, respectively.

Therefore, the total force on the BM F_{BM} is given by:

$$F_{\text{BM}} = p(x,0,t) + F_{\text{cell}}(x,t).$$

Due to the longitudinal tilt of OHC, forces acting on the cilia at x cause OHC to push at a point $x+\Delta$ downstream on the BM. Hence:

$$F_{\text{cell}}(x+\Delta,t) = \alpha(u,x,t)F_{\text{BM}} = \alpha(u,x,t)\big(p(x,0,t) + F_{\text{cell}}(x,t)\big)$$

α, i.e. the *gain factor*, has an integral form shown in the next paragraph (see 3.5).

OHC saturate as the BM motion increases in magnitude, thus α has in fact a nonlocal and nonlinear expression which depends on the history of $u(x,t)$, i.e. the BM displacement (see [10], Fig. 3).

By modeling BM motion as a spring-mass system and setting $F_{\text{cell}}(x,t) =: q(x,t)$, the active model becomes:

$$\begin{cases} \mathbf{\Delta} p(x,z,t) = 0, & (x,z) \in [0,L] \times [0,H], \\ p(x,0,t) + q(x,t) = mu_{tt} + ru_t + s(x)u, & 0 \leqslant x \leqslant L, \\ q(x+\Delta,t) = \alpha(x,u,t)\big(p(x,0,t) + q(x,t)\big), & 0 \leqslant x \leqslant L - \Delta, \\ q(x,t) = 0, & 0 \leqslant x \leqslant \Delta, \end{cases} \tag{1}$$

where $\mathbf{\Delta}$ is the Laplacian operator, and the initial-boundary conditions are the same of the classical passive model.

More precisely, the external stimulus is present in

$$p_x(0,z,t) = 2\rho T_m sp_{\text{input}}(t), \quad 0 \leqslant z \leqslant H,$$

where $T_m sp_{\text{input}}$ includes medium ear's mechanical effects. Moreover, being the equations in p coupled through u, i.e. the BM displacement, it follows

$$p_z(x,0,t) = 2\rho u_{tt}(x,t), \quad 0 \leqslant x \leqslant L.$$

The other two boundary conditions are

$$\partial p(x,H,t)/\partial z = 0, \quad 0 \leqslant x \leqslant L$$

a homogeneous Neumann bc because the upper wall is rigid;

$$p(L,z,t) = 0, \quad 0 \leqslant z \leqslant H.$$

The initial conditions are

$$u(x,0) = 0, \qquad \frac{\partial}{\partial t} u(x,0) = 0, \quad 0 \leqslant x \leqslant L.$$

3. The existing discrete 2D–1D model with a nonlocal gain factor

The semidiscrete model discussed here is considered in [10] and is a 2D model reduced to a 1D one by concentrating the attention on the movement of BM. The authors consider a uniform mesh on the rectified model of the BM with $N+1$ nodes x_i, $i = 0,\dots,N$ and $x_i = i \cdot \Delta x$ so that $u(x_i,t)$ represents $u(i\Delta x,t)$, $i = 0,\dots,N$, $\Delta x = L/N$, being L the length of the BM.

By expanding p by the eigenfunctions of the Laplacian and after posing

$$Q(t) = \big[q(x_0,t)\dots q(x_N,t)\big]^T, \qquad P(t) = \big[p(x_0,t)\dots p(x_N,t)\big]^T,$$
$$F(t) = 2\rho T_m p_t(t)\big[(L-x_0)\dots(L-x_N)\big]^T,$$

and some manipulation on (1) (see [10]) the model (1) can be reduced to a semidiscrete one, a sequence of initial value problem based on systems of $N+1$ second order differential equations parametrized by Δx:

$$M\frac{\partial}{\partial t^2}U = r\frac{\partial}{\partial t}U + SU + \big(B^{-1}C + I\big)F, \qquad U(0) \text{ and } \frac{\partial}{\partial t}U(0) \text{ given,} \tag{2}$$

where r is the resistance and the $(N+1)\times(N+1)$ mass matrix M is given by

$$M = M(U) = \big(B^{-1}C + I\big)A - mI, \qquad B = B(U), \qquad C = C(U), \tag{3}$$

being m the BM density, S a diagonal matrix given by the BM stiffness per unit length in the form

$$s(x) = 4\pi^2 m\big(0.456\exp\big(4.83(1-x/L)\big) - 0.45\big)^2,$$

$$B = \begin{pmatrix} 1 & & & & & & & \\ 0 & 1 & & & & & & \\ \vdots & \ddots & & & & & & \\ \vdots & \ddots & \ddots & & & & & \\ -\alpha(x_0,u) & & & 1 & & & & \\ & \ddots & & 0 & 1 & & & \\ & & & & \ddots & \ddots & & \\ & & -\alpha(x_{N-K},u) & 0 & \dots & 0 & 1 & \end{pmatrix}, \tag{4}$$

i.e., $B_{i+K,i} = -\alpha(x_i, u, t)$, $i = 0, \ldots, N-K$, $K = 1$ in [10] and in our settings, $C = -B + I$ and $A = (a_{i,j})$ is the nonsymmetric matrix generated by the Laplacian eigenfunction expansion

$$a_{i,j} = \sum_{n=1}^{m} \frac{-4\rho\cos(\xi_n x_i)\cos(\xi_n x_j)}{L\xi_n \tanh(\xi_n H)} d(j)\Delta x, \quad i, j = 0, \ldots, N, \tag{5}$$

$d(j) = 1$ on interior points and $1/2$ at the end points, H is the height of the cochlea, $\xi_n = \pi(n - 0.5)/L$. The *gain factor* $\alpha = \alpha(x, u, t)$ is a nonlocal nonlinear function that in [10] is defined as

$$\alpha(x, u, t) = \frac{\gamma}{\sqrt{\lambda\pi}} \int_0^L \exp\left(-\frac{(x - x')^2}{\lambda}\right) g\big(u(x', t)\big)\, dx', \tag{6}$$

where λ, γ are constants and g is a nonlinear function; see [10] for details. In this paper we propose an extension to this function. Note that the entries of A do not change and depend only on the mesh.

In [10] the authors reduce (2) to a system of $2(N+1)$ first order equations and by using the well known 2-step BDF formula (see, e.g., [8]), they derive two systems of $N+1$ difference equations

$$U^{n+2} = \frac{4}{3}U^{n+1} - \frac{1}{3}U^n + \frac{2}{3}\Delta t V^{n+2}, \tag{7}$$

$$V^{n+2} = \frac{4}{3}V^{n+1} - \frac{1}{3}U^n + \frac{2}{3}\Delta t \big(M^{n+2}\big)^{-1}\big(rV^{n+2} + SU^{n+2} + \big(\big(B^{n+2}\big)^{-1}C + I\big)F^{n+2}\big), \tag{8}$$

where, incidentally, also M, B and C do depend on U^{n+2}.

By using (7) in (8) one obtains:

$$\begin{aligned}&\left(M^{n+2} - \frac{2}{3}\Delta t\, rI - \left(\frac{2}{3}\Delta t\right)^2 S\right)V^{n+2}\\ &\quad = M^{n+2}\left(\frac{4}{3}V^{n+1} - \frac{1}{3}V^n\right) + \frac{2}{3}\Delta t\left(S\left(\frac{4}{3}U^{n+1} - \frac{1}{3}U^n\right) + \big(\big(B^{n+2}\big)^{-1}C + I\big)F^{n+2}\right).\end{aligned} \tag{9}$$

Therefore, the mass matrix is given by

$$\tilde{M}^{n+2} := M^{n+2} - \frac{2}{3}\Delta t\, rI - \left(\frac{2}{3}\Delta t\right)^2 S = \big(B^{n+2}\big)^{-1}A - \tilde{D}, \tag{10}$$

where B^{n+2} is a 2-band matrix (lower bidiagonal if $K = 1$, the choice in [10] and here), A is a (fixed once Δx is fixed) full matrix and $\tilde{D}$ is a diagonal matrix:

$$\tilde{D} = mI + \frac{2}{3}\Delta t\, rI + \left(\frac{2}{3}\Delta t\right)^2 S$$

and only B^{n+2} depends on u via the gain factor α.

4. Our proposal to adapt the discrete model to patients with SHL

In the next paragraphs we propose some changes to the strategies in [10] in order to get a discrete model that can

- describe more accurately SHL and hyperacusis with unconditional convergence to an approximate solution;
- be computationally robust and efficient.

Simulations and more details on the computational methods will be considered in Section 5.

4.1. Time marching schemes

Instead of using 2-step BDF, we suggest two options. The first one is a scheme to be used with constant stepsize, see Section 4.1.1. The second one is a variable step with variable order package for time-step integration based on *Matlab*'s `ode15s`. Indeed, we modified the latter algorithm in order to accommodate the use of an iterative solver for the linear algebraic systems and to consider the peculiar structure of the mass matrix of the semidiscrete model; see Section 4.1.2.

4.1.1. Constant stepsize and order time stepping

We propose using an order two difference scheme for (2) (reduced to a first order sequence of differential equation parametrized by Δt), i.e. *Crank–Nicolson* (CN). Our proposal tries to contribute for two main reasons:

- CN is A-stable and does not smooth unstable modes as L-stable methods as 2-step BDF do (see, e.g., [8]);
- is a one-step method, therefore change of the stepsize is more natural.

Applying CN to (2) after some manipulations gives

$$U^{n+1} = U^n + \frac{1}{2}\Delta t\big(V^n + V^{n+1}\big), \tag{11}$$

$$MV^{n+1} = MV^n + \frac{1}{2}\Delta t\big\{r\big(V^n + V^{n+1}\big) + S\big(U^n + U^{n+1}\big) + \big(B^n\big)^{-1}F^n + \big(B^{n+1}\big)^{-1}F^{n+1}\big\}. \tag{12}$$

By substituting (11) in (12) and by recalling that $B^{-1}C + I = B^{-1}$, gives

$$\left(M - \frac{1}{2}\Delta t\, rI - \left(\frac{1}{2}\Delta t\right)^2 S\right)V^{n+1} = \left\{M + \frac{1}{2}\Delta t(rI + S)\right\}V^n + \Delta t\, U^n + \frac{1}{2}\,\Delta t S\big(\big(B^n\big)^{-1}F^n + \big(B^{n+1}\big)^{-1}F^{n+1}\big). \tag{13}$$

Now the *mass matrix* is given by

$$\tilde{M}^{n+1} := M^{n+1} - \frac{1}{2}\Delta t\, rI - \left(\frac{1}{2}\Delta t\right)^2 S = \big(B^{n+1}\big)^{-1}A - \tilde{D}, \tag{14}$$

where the changes with other multistep schemes are confined in the diagonal term $\tilde{D}$ in (14).

The discrete problem (13) can be reduced to a linearized one by approximating the values of the gain factor $\alpha(u(x,t))$ in B (and then in C too) by using Taylor series expansion:

$$U^{n+1} = U^n + \Delta t\, V^n + \frac{1}{2}\,\Delta t\big(V^n - V^{n-1}\big) + O\big((\Delta t)^3\big), \quad n = 1, 2, \ldots, \tag{15}$$

by including in the first step a first order expansion as $U^{n+1} = U^n + \Delta t\, V^n$ in order to start the process.

4.1.2. Variable stepsize and order time stepping

In order to get a more effective time-step integration, we modified the variable step, variable order (from order 1 to five) package `ode15s` based on NDF formulas included in release 2008b of *Matlab*; see [18]. For details of iterative solution of the algebraic linear systems in `ode15s` see [2]. In order to use the above strategy, we perform three steps:

- reduce (2) to first order system of differential equations;
- reduce the solution of each $2(N+1)$ linear algebraic system to the solution of one $N+1$ linear system;
- use an iterative Krylov solver for the solution of the latter system.

We first reduced the second order system (2) to a first order one

$$\begin{pmatrix} I & 0 \\ 0 & M \end{pmatrix}\begin{pmatrix} U \\ V \end{pmatrix}' = \begin{pmatrix} 0 & I \\ S & rI \end{pmatrix}\begin{pmatrix} U \\ V \end{pmatrix} + \begin{pmatrix} 0 \\ B^{-1}F(t) \end{pmatrix} \tag{16}$$

where we recall that the mass matrix M is given by

$$B^{-1}A - mI$$

and every operation requires a full matrix computation because of A. On the other hand, the Jacobian matrix of (16) is sparse and constant. In particular, it can be viewed as a 2×2-block matrix whose four blocks are $N+1 \times N+1$ diagonal or null. In order to avoid the solution of linear(ized) systems of $2(N+1)$ equations, we can observe that the matrices of these algebraic systems can be written as

$$\mathcal{A} = \mathcal{M} - \Delta t \cdot a \cdot \mathcal{J}, \tag{17}$$

where $\mathcal{M}$, $\mathcal{J}$ are the mass and the Jacobian matrix in (16), respectively and Δ_t, a are scalars, i.e. the stepsize and a parameter that can be different for each time step. Therefore, with the notation

$$\mathcal{A} = \begin{pmatrix} \mathcal{A}_1 & \mathcal{A}_2 \\ \mathcal{A}_3 & \mathcal{A}_4 \end{pmatrix} \tag{18}$$

we immediately get that $\mathcal{A}_1$, $\mathcal{A}_2$ and $\mathcal{A}_3$ are $N+1 \times N+1$ diagonal matrices, while $\mathcal{A}_4$ is $N+1 \times N+1$ and full. Moreover, after a few manipulations, we get that the solution of linear systems whose matrices have same structure as $\mathcal{A}$ is given by solving the system

$$\big(\mathcal{A}_4 - \mathcal{A}_3\mathcal{A}_1^{-1}\mathcal{A}_2\big)x_2 = b_2 - \mathcal{A}_3\mathcal{A}_1^{-1}b_1 \tag{19}$$

Table 1
dB SPL–dB HL conversion formula.

kHz	dB SPL	dB HL
0.25	11.7	0
0.5	3.5	0
1	0	0
2	0	0
3	0	0
4	0	0
6	0	0
8	5	0

and then by computing directly

$$x_1 = \mathcal{A}_1^{-1} b_1 - \mathcal{A}_1^{-1} \mathcal{A}_2 x_2, \tag{20}$$

where x_1, b_1 and x_2, b_2 are the first $N+1$ and the last $N+1$ entries of the solution vector x and of the right hand side b of the linear system $\mathcal{A}x = b$, respectively. It is worth to note that the matrix inversions of $\mathcal{A}_1$ in (20) and (19) are trivial because $\mathcal{A}_1$ is diagonal.

Due to the special spectral properties of the matrix $\mathcal{A}$ of the underlying linear systems, in order to reduce the computational complexity (both in space and time), we can use a Krylov subspace iterative solver instead of a direct one for (19) whenever N is large, as detailed in Section 4.3 (see also [2]).

4.2. A gain factor tuned for SHL with OHC damage

As observed in the Introduction, we will show here that the gain factor $\alpha = \alpha(x, u, t)$ can assume values greater than one in case of hypoacusia due to OHC damage with intact IHC and, in particular, whenever recruitment and hyperacusis act in suitable dB-ranges.

The crucial point is that a realistic reproduction of the SHL in the latter situation cannot be described by the expression (6). More precisely, the profile of α vs. the BM displacement u and the associated SHL curves for the corresponding values of the gain constant γ in (6) (see [11], Fig. 1 to Fig. 4) can be applied only to patients with normal hearing ($\gamma = 0.52$) or, at most, with mild SHL ($\gamma \geqslant 0.4$). As a matter of fact, the medical experience (see [14]) clearly shows that a deafness characterized by intact IHC induces a maximum SHL of 50–60 dB and a painful hyperacusis above a sound level of 80–90 dB. We stress that, since the model in [11] does not take into consideration IHC, severe SHL (even if limited to the high frequencies!) cannot be investigated by the latter model.

Furthermore, it is important to emphasize that, although a great amount of the compressive nonlinearity of a normal ear is destroyed in an impaired ear with moderate SHL, the real behavior of the auditive perception cannot be described by a linear model based only on the BM displacement vs. the input level, i.e. the passive model (see [11], Fig. 2).

In case of moderate or mild to moderate SHL ($\leqslant 60$ dB HL), the main effect is, in fact, a strong reduction of the dynamical auditive range from 0–100 dB HL of normal hearing to 25–30 dB above hearing threshold of an impaired ear.

From a medical point of view, it is not clear the origin of hyperacusis in an impaired ear with a moderate SHL. There are several theories trying to explain the latter phenomenon by an abnormal reaction of the central auditive pathways and, more precisely, by considering the neural connections of the so-called cochlear nuclei with *a strong subjective component*. Sound enrichment therapies are in fact useful in many cases to deal with this pathology.

On the other hand, other interpretations are referred to in the literature and include hyperactivity of afferent and/or efferent connections, over-reactions of residual OHC or even sudden vibrations of BM often associated to subjective tinnitus (see [13] and the cited references). Since no appropriate imaging techniques are available for the human ear, we assume that *hyperacusis can be measured by a BM-displacement in nm-equivalent*.

Hence, in case of a complete loss of OHC ($\gamma = 0$) and by considering the same input frequencies chosen in [11], Fig. 2, i.e. 0.5 kHz, 2 kHz, 6 kHz, the following values can be deduced by medical experience (see Fig. 1):

(a) by assuming a SHL of 50 dB at 2 kHz and a SHL of 60 dB at 6 kHz, hyperacusis starts around 85–90 dB SPL in both cases,
(b) recruitment is already present at 75–80 dB SPL in both frequencies,
(c) at 0.5 kHz with a SHL of 35 dB SPL recruitment is practically absent and hyperacusis starts at 95 dB SPL, i.e. it is almost equivalent to the recruitment of loudness of a sensible normal ear.

The (linear) conversion formula from dB HL to dB SPL is displayed in Table 1.

Therefore, the theoretical gain factor α is affected by an amplification factor induced both by hyperacusis and by recruitment. In conclusion, audiological experience shows that *an impaired ear with a SHL $\leqslant 60$ dB is definitely a nonlinear and active system at least in a suitable range of values*.

From a mathematical point of view, hyperacusis can be described by *the nonlinear gain factor* $\tilde{\alpha}$. More precisely, $\tilde{\alpha}(x, u(x, dB(t))$ is a sigmoid function both of the tonotopic site x and of the BM-displacement u in *nm*-equivalent, asso-

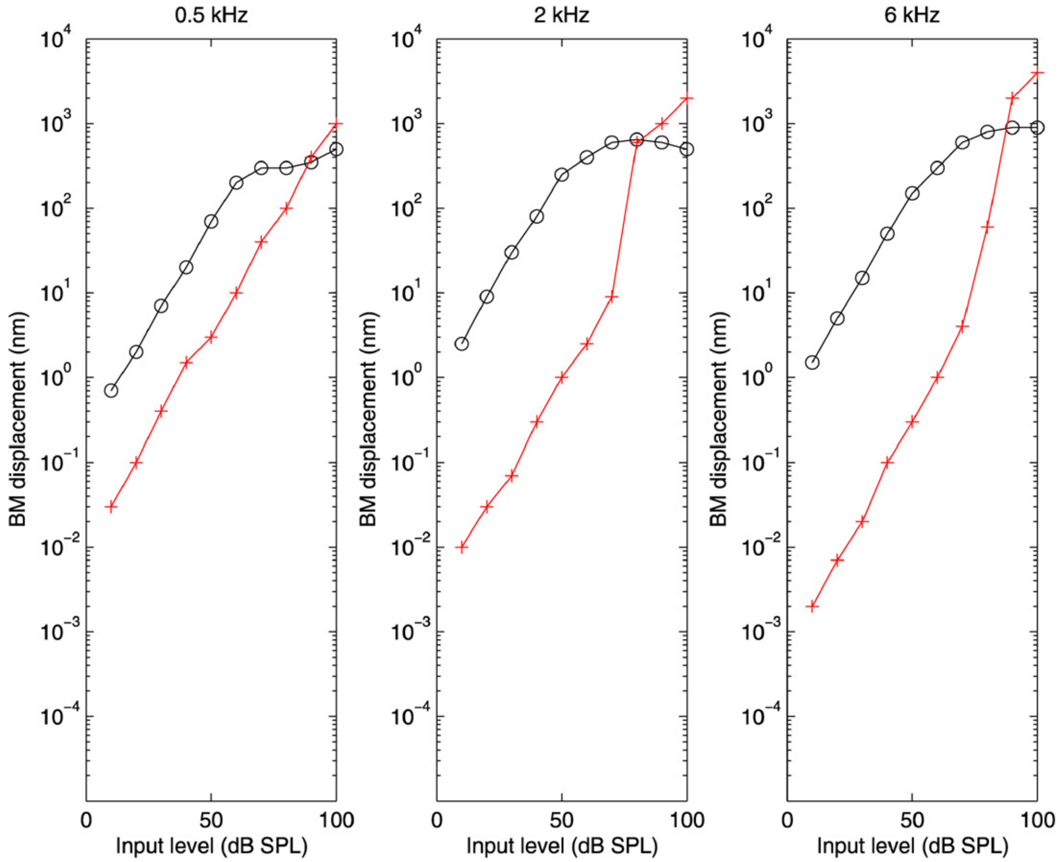

Fig. 1. BM-displacement for normal (line-circle, $\gamma = 0.52$) and impaired (line-plus, $\gamma = 0$) ears.

ciated to the input level of the signal in dB SPL. The latter assumption can be explained by interpreting hyperacusis as a sort of overreaction to a neural excitation. The analysis of samples of audiological data confirms that a realistic model of recruitment and hyperacusis can be obtained by adding to the gain factor $\alpha(x,u,t)$ in (6) a new nonlinear component $\tilde\alpha = \tilde\alpha(x, u(x, dB(t))$ depicted in Fig. 2 for the tonotopic sites x associated to 2 kHz and 6 kHz.

So, *the total gain factor* $\hat\alpha$ is given by:

$$\hat\alpha(x,u,t) = \frac{\gamma}{\sqrt{\lambda\pi}} \int_0^L \exp\left(-\frac{(x-x')^2}{\lambda}\right) g\big(u(x',t)\big)\,dx' + \tilde\alpha\big(x, u\big(x, dB(t)\big)\big) \tag{21}$$

where $\lambda = 0.01$ cm^2 and γ is the gain constant associated to the level of SHL.

We point out that when $u(x, dB(t)) > 250$ nm the theoretical local gain factor $\alpha = 0$, thereby implying $\hat\alpha = \tilde\alpha$ (see [11], Fig. 1). Moreover, by applying (21), we can immediately deduce that $\tilde\alpha > 1$ in a suitable range of values of the input signal, depending on the frequency associated to the tonotopic site x.

By utilizing the *line-plus* curves depicted in Fig. 1, referred to the frequencies 0.5 kHz, 2 kHz, 6 kHz and by denoting with *IL* the input level, one can obtain the following results (see Fig. 2):

(i) at 0.5 kHz, since hyperacusis starts at 95 dB, $\tilde\alpha < 1$ for $IL < 100$ dB,
(ii) at 2 kHz and 6 kHz $0 < \tilde\alpha < 1$ for $70 < IL \leqslant 85$ dB, $\tilde\alpha > 1$ for $IL > 85$ dB,
(iii) the growth of $\tilde\alpha$ for $IL > 85$ dB is much stronger at 6 kHz than at 2 kHz ($\tilde\alpha > 4.5$ for $IL = 100$ dB).

4.3. Krylov subspace methods for the system of algebraic equations

Solving the solution of the discrete models we consider in this paper requires the solution of a linear system for each time step, see (11), (12), (19). Differently to [10], we propose the use of *projection methods* like BiCGStab and GMRES; see, e.g., [16] for a review.

Krylov subspace methods are used here as iterative solvers, i.e., given an initial approximate solution x_0, these algorithms compute a sequence of approximations. *Krylov subspace* iterative linear solvers at each iteration seek a new approximate

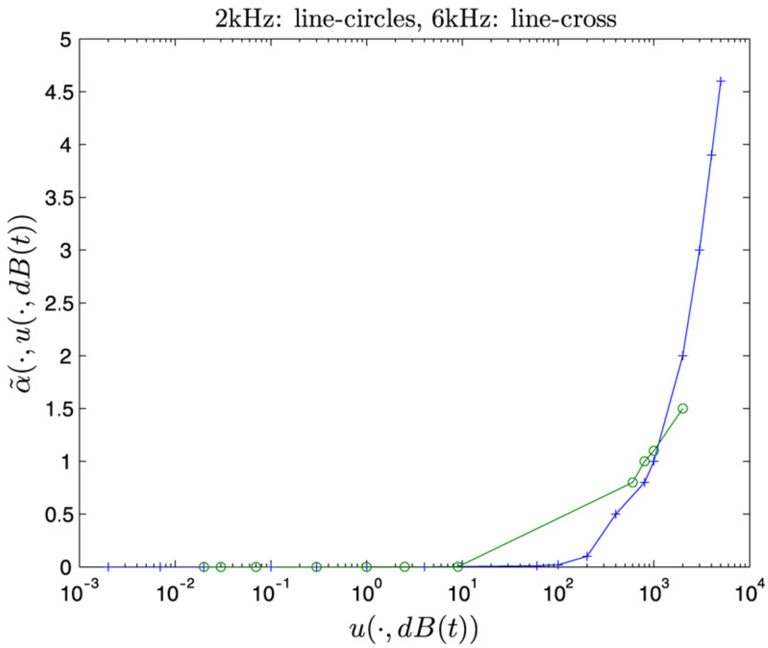

Fig. 2. $\tilde{\alpha}$ vs BM-displacement for 2 kHz (line-circle) and 6 kHz (line-cross).

solution in the affine subspace $x_0 + K_m$, where x_0 is an initial guess and K_m is the *Krylov* subspace of $\mathbb{R}^n$ of dimension $m \leqslant n$:

$$K_m = \text{span}\{v, \tilde{M}v, \tilde{M}^2 v, \ldots, \tilde{M}^{m-1} v\}.$$

Here $\tilde{M}$ is the coefficient matrix of the linear system that we want to solve and v is a vector related to the initial residual vector. The (unique) approximation x_m at step m is computed by using an orthonormal basis for K_m determined during the iteration steps. More specifically, the next residual vector is constrained to be orthogonal to m linearly independent vectors defining a subspace L_m of dimension m, which is called the subspace of constraints. The choice of subspaces varies for different Krylov subspace linear system solvers. This framework is known as the Petrov–Galerkin conditions (see [16, Chapter 6] for details).

We recall that projection methods can converge faster whenever the matrix of the underlying linear system presents a cluster of eigenvalues in one of the half complex plane (see, e.g., [4]). Indeed, we experienced that the matrix of linear systems in (19) shows a cluster of eigenvalues in the left half plane; see Figs. 3 and 4. Moreover, differently to the fixed point iterative method proposed in [10], we have unconditional convergence, in particular with respect to the time step and to the values of α without artificial restrictions. This is very important in order to

- allow the use of adaptive time steps not limited by stability reasons;
- converge even when hyperacusis is acting, i.e. in the case $\tilde{\alpha} > 1$.

4.4. Hyperacusis and ill-conditioning of the discrete model

In this paragraph we will prove that hyperacusis can imply the ill-conditioning of matrix B in (14) and (16) (and of course in (10) and (19)) in a nonempty (discrete) frequencies interval. We stress that the latter matrix is of crucial importance in the computation in the framework proposed in [10]. Moreover, the solution of linear systems containing the matrix B must be carefully dealt with from a computational point of view. The generation of the matrix–vector product with M or $\tilde{M}$, i.e. at each iteration of projective algorithms like Krylov subspace methods, is in fact a critical problem. In Section 4.2 it was shown that the new gain factor $\tilde{\alpha}$ can assume values greater than one in the tonotopic sites associated to frequencies greater or equal to 2 kHz and for suitable dB-ranges.

In order to obtain a numerical interpretation of a sensorineural overreaction we must take into account some anatomical characteristics of the Organ of Corti. In absence of appropriate imaging techniques a natural way to describe the complex phenomena associated to hyperacusis is to *assume that the electromechanical processing performed by* OHC *in an impaired ear can be considered equivalent to an unstable parassitary term affecting the true solution of a normal ear.*

By utilizing the strategies suggested in the present paper, the following questions arise: does hyperacusis imply a sort of numerical instability of (2) and, consequently, of the corresponding approximation? In the affirmative, is the matrix B involved in the computation ill-conditioned?

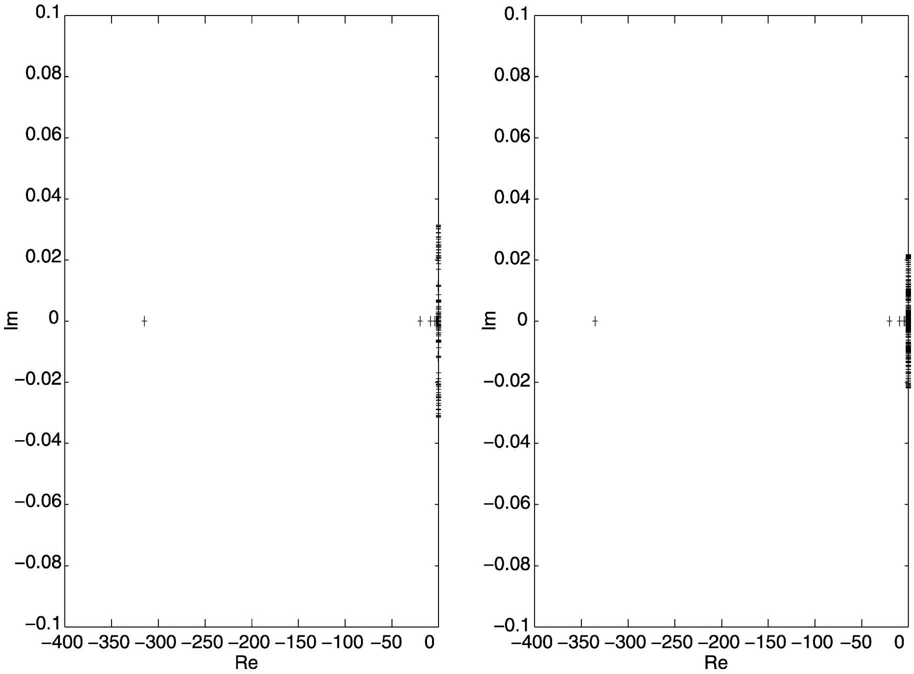

Fig. 3. (From left to right.) Spectrum of matrix in (19), $N = 150$ and $N = 300$.

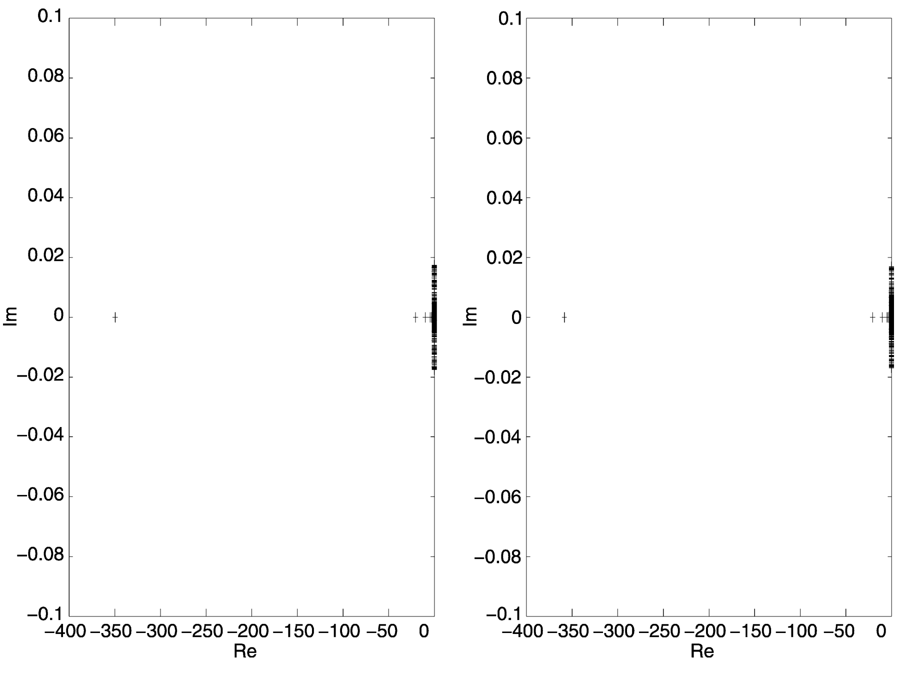

Fig. 4. (From left to right.) Spectrum of matrix in (19), $N = 600$ and $N = 1200$.

Let us suppose that B, which is a lower bidiagonal matrix, be reducible, i.e., there exist zero entries in its nontrivial subdiagonal so that we can write B as

$$B = \begin{pmatrix} I_k & & \\ & B_{22} & \\ & & I_{N+1-k-s} \end{pmatrix}. \tag{22}$$

We get that

$$\kappa_p(B) = \|B_{22}\|_p \left\|(B_{22})^{-1}\right\|_p,$$

where $\kappa_p(B)$ is the *condition number* of B with respect to the p-norm, $\|\cdot\|_p$ is an operator norm and B_{22} can be written as

$$B_{22} = \begin{pmatrix} 1 & & & & \\ a_{k+1} & 1 & & & \\ & a_{k+2} & 1 & & \\ & & \ddots & \ddots & \\ & & & \ddots & 1 \end{pmatrix},$$

B_{22} is the submatrix of B corresponding to the interval

$$x \in [x_k, x_{k+s-1}] \in [0, L],$$

I_* are identity matrices of suitable order. Therefore, without leading generality, we can assume that B is an $(N+1)\times(N+1)$ irreducible lower bidiagonal matrix with $a_j > 0$ for all $j = 0, \ldots, N$.

Proposition 1.

$$\kappa_p(B) \geqslant c \prod_{j\in\mathcal{J}} a_j, \tag{23}$$

where $\mathcal{J}$ is the set of indexes such that $\forall j \in \mathcal{J} \subseteq \{0, 1, 2, \ldots, N\}$, $a_j > 1$ and c is a constant.

Proof. Let us suppose $\hat{\alpha} > 0$ for all $x \in [0, L]$, otherwise we can split B as in (22). Moreover, let x_k be the first point of the mesh on the BM where $\tilde{\alpha}$ is greater than one. By writing out the $N+1$ equations in $Bx = b$ where

$$b = [0 \ldots 0\ 1\ 0 \ldots 0]^T$$

is the k-vector of the canonical basis of $\mathbb{R}^{N+1}$ we get

$$x_0 = 0, \quad a_1x_0 + x_1 = 0, \quad \ldots, \quad a_kx_{k-1} + x_k = 1, \quad a_{k+1}x_k + x_{k+1} = 0, \quad a_Nx_{N-1} + x_N = 0$$

and therefore

$$x_1 = 0, \quad \ldots, \quad x_k = 1, \quad \ldots, \quad x_{k+1} = a_{k+1}, \quad x_{k+2} = a_{k+1}a_{k+2}, \quad \ldots.$$

From $Bx = b$

$$\|x\| \leqslant \|B^{-1}\| \cdot \|b\| \quad \Rightarrow \quad \|B^{-1}\| \geqslant \frac{\|x\|}{\|b\|},$$

and, if $\mathcal{J}$ is the set of indexes such that $\forall j \in \mathcal{J} \subseteq \{0, 1, 2, \ldots, N\}$ we have $a_j > 1$,

$$\|x\|_\infty \geqslant \prod_{j\in\mathcal{J}} a_j. \tag{24}$$

This, since $\|b\| = 1$, reads

$$\|B^{-1}\|_\infty \geqslant \prod_{j\in\mathcal{J}} a_j.$$

The proof is completed by including in a constant c in (23) the p-norm of B and a weight factor dependent on the operator norm used. □

We stress that ill-conditioning is with respect to the mesh parameter Δx refinements. In Tables 2–4 we give a sample of the condition numbers related to three different situations. As expected, condition numbers of the matrices

- B as in (4),
- the mass matrix $M = GA - mI$ as in (3),
- the matrix $\mathcal{C} = \mathcal{A}_4 - \mathcal{A}_3\mathcal{A}_1^{-1}\mathcal{A}_2$ of the linear system (19),

grow fast with $\max\{\tilde{\alpha}\}$. This suggests to build up another new model for a cochlea affected by a sensorineural hearing loss. We plan to take care of this in a future work. Values greater than $1/eps$ are not reported in Table 4 for $N = 200$ and $N = 500$, where eps is the machine precision.

Table 2
Condition number of matrix B as in (4) and mass matrix $M = GA - mI$ as in (3) for $\max\{\tilde{\alpha}\} \leqslant 1$.

N	$K_\infty(B)$	$K_\infty(M)$	$K_\infty(\mathcal{C})$
50	13	4787	4600
100	17	5130	12 600
200	22	6680	20 370
500	28	8800	35 140

Table 3
Condition number of matrix B as in (4) and mass matrix $M = GA - mI$ as in (3) for $\max\{\tilde{\alpha}\} \leqslant 1.2$.

N	$K_\infty(B)$	$K_\infty(M)$	$K_\infty(\mathcal{C})$
50	45	11 470	32 100
100	129	22 240	93 876
200	713	110 880	746 920
500	70 774	9 310 690	103 602 500

Table 4
Condition number of matrix B as in (4) and mass matrix $M = GA - mI$ as in (3) for $\max\{\tilde{\alpha}\} \leqslant 2.4$.

N	$K_\infty(B)$	$K_\infty(M)$	$K_\infty(\mathcal{C})$
50	4.5×10^6	5.44×10^8	1.47×10^9
100	1.19×10^{12}	1.6×10^{14}	7.14×10^{14}
200	–	–	–
500	–	–	–

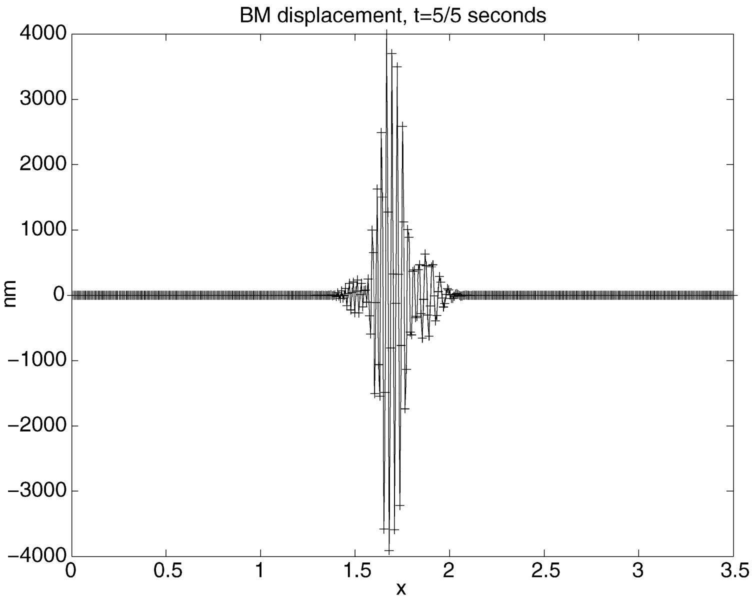

Fig. 5. BM displacement with input stimulus 4 kHz at 90 dB for an impaired ear.

5. Numerical experiments

In this section some preliminary numerical experiments are reported by using a variable step-variable order Matlab package based on implicit formulas modified in part in the style of [2] with iterative solution of the linear algebraic systems. Moreover, we adapt the package for the use with system with a nontrivial 2×2 block mass matrix showing the structure discussed in Section 4.1.2. To compare results with those given in [10], we considered $\tilde{\alpha}$ depending only on x. In Fig. 5 we can see an example of BM displacement for impaired ear; see Section 4.2 for details on the gain factor. The input signal is sinusoidal, frequency is 4 kHz at 90 dB. The simulation was performed by using $N = 500$ discrete points on the BM, but no appreciable difference is shown with, e.g., $N = 250$ or $N = 2000$. The maximum value of the gain factor $\tilde{\alpha}$ is greater than 1 and hyperacusis is in force. This is in agreement with the clinical data.

In order to speed up the proposed numerical methods, we used Krylov subspace solvers. In particular, both GMRES and BiCGStab were considered with similar results; see [16] for details on these iterative methods. The convergence to the

Table 5
Convergence ratios in L_2 and L_∞ norms.

N	$\|u_N - u_{2N}\|/\|u_{2N} - u_{4N}\|_2$	$\|u_N - u_{2N}\|/\|u_{2N} - u_{4N}\|_\infty$
250	4.12	3.76
500	4	3.9

prescribed tolerance of the former and the latter were reached in a number of iteration not increasing with N, as expected by the clustered spectra observed in Section 4.3, typically 30–50 without preconditioning for a tolerance with respect to the relative residual of 10^{-9}. However, a preconditioning strategy can be designed by using updated incomplete factorizations described in [1]. We experienced a computing time of less than 10' minutes (compare with 25' of [10]) on a Pentium IV laptop for $N = 700$, continuous input frequency of 4 kHz and a relative error estimate in 2-norm solution (i.e. w.r.t. the solution of (16)) of 10^{-3} (no error estimation in [10]). In particular, the average time step Δt was of the order of 10^{-5} to get a 30/40 ms simulation. We stress that this time can be reduced by implementing efficiently our strategies in a compiled language. However, this is beyond the scope of this presentation.

We test the convergence of the proposed scheme by showing ratios $\|u_N - u_{2N}\|/\|u_{2N} - u_{4N}\|_2$ for $N = 250$ and $N = 500$. It is worth to remind that, differently to the tests performed in [10], we are using an automatic variable step and order package in our numerical experiments. Table 5 confirms that the scheme is a globally second order one for the discretization with respect to the space variables. This upper limit is mainly caused by the use of the *trapezoidal rule*, which is a second order quadrature formula, to form matrix A as in (5); see [10].

As a final note, the convergence of the whole scheme does not depend on the size of $\tilde{\alpha}$ or α or on the step sizes, differently to the strategy proposed in [10], where the fixed point iterative solver was proved to converge only if $\alpha < 1$, and if the stepsize in time was small enough; see [10, page 689]. On the other hand, values of α that are larger than 1 give ill-conditioning for mass and B matrices. This is certainly a limit of the model proposed in [10] and extended here for an impaired inner ear.

6. Conclusions

In this work we have shown that the numerical solution of integro-differential equations associated to the modeling of an impaired ear with OHC damage presents several difficulties.

First, although a great amount of the nonlinearity is lost in case of moderate SHL, the classical linear passive model cannot be applied in the latter situation.

Second, fixed time-step integration algorithm requires quite small time steps in order to ensure the convergence and the same precision that can be reached by an adaptive time-step integration, as the one we suggest in Section 4.1.2. Consequently, there is a risk of a significant waste of computational resources. The use of a Matlab package based on implicit formulas for time-step integration suitably modified for the use of iterative solvers can be recommended for the nature of the considered model, robust and relatively simple to accommodate the changes of an external user.

Moreover, when the number of mesh points N is large, in order to avoid matrix factorizations, an iterative linear algebraic system solver can be more appropriate than a direct one for solving discrete problems generated by implicit time stepping. However, the use of a fixed point iterative algorithm gives conditional convergence, thereby suggesting the utilization of projection methods.

Third, recruitment and hyperacusis can imply the ill-conditioning of the discrete model at least in a suitable range of dB-values.

Preliminary numerical results and simulations, illustrated in Section 5, confirm the theoretical unconditional convergence of the computational scheme and the expected behavior in case of hyper/hypoacusia. We plan to give more simulations and results in a forthcoming paper.

Acknowledgements

The authors would like to thank the anonymous referees for helpful comments and useful suggestions which have improved this presentation.

References

[1] D. Bertaccini, Efficient solvers for sequences of complex symmetric linear systems, ETNA 18 (2004) 49–64.
[2] D. Bertaccini, D. Calvetti, Fast simulation of solid tumors thermal ablation treatments with a 3D reaction diffusion model, J. Comp. Biol. Med. 37 (2007) 1173–1182.
[3] E. De Boer, Mechanics of the cochlea: Modeling efforts, in: The Cochlea, in: Springer Handbook of Auditory Research, vol. 8, Springer-Verlag, New York, 1996, pp. 258–317.
[4] A. Greenbaum, Iterative Methods for Solving Linear Systems, SIAM, Philadelphia, 1997.
[5] M. Holmes, J.D. Cole, Cochlear mechanics: Analysis for a pure tone, J. Acoustic Soc. Amer. 76 (1984) 767–778.
[6] A. Inselberg, Cochlear dynamics: The evolution of a mathematical model, SIAM Rev. 20 (2) (1978) 301–351.
[7] A. Inselberg, R.S. Chadwick, Mathematical model of the Cochlea. I: Formulation and solution, SIAM J. Appl. Maths. 30 (1) (1976) 149–163.

[8] J.D. Lambert, Numerical Methods for Ordinary Differential Systems, John Wiley & Sons, Chichester, 1991.
[9] H. Kim, D.M. Barrs, Hearing aids: A review of what's new, Otolaryngology-Head and Neck Surgery 134 (6) (2006) 1043–1050.
[10] Y. Kim, J. Xin, A two-dimensional nonlinear nonlocal feed-forward cochlear model and time domain computation of multitone interactions, Multiscale Model. Simul. 4 (2) (2005) 664–690.
[11] Y. Kim, J. Xin, Y. Qi, A study of hearing aid gain functions based on a nonlinear nonlocal feedforward cochlea model, Hearing Res. 215 (2006) 84–96.
[12] K.M. Lim, C.R. Steele, A three dimensional nonlinear active cochlear model analyzed by the WKB-numeric method, Hearing Res. 170 (2002) 190–205.
[13] A.R. Moeller, Neural plasticity in tinnitus, Progr. Brain Res. 157 (2006) 365–372.
[14] R. Pujol, IA:, http://www.iurc.montp.inserm.fr/cric51/audition/english/pathology/, Promenade around the Cochlea: Pathology of hair cells and neurons.
[15] R. Pujol, J.L. Puel, Excitotoxicity, synaptic repair, and functional recovery in the mammalian cochlea: A review of recent findings, Ann. New York Acad. Sci. 884 (1) (1999) 249–254.
[16] Y. Saad, Iterative Methods for Sparse Linear Systems, PWS Publishing Company, Boston, MA, 1995.
[17] G. Von Bèkèsy, Concerning the pleasures of observing and the mechanics of the inner ear, Nobel Lecture, Dec. 11th 1961.
[18] L.F. Shampine, M.W. Reichelt, The MATLAB ODE suite, SIAM J. Sci. Comput. 18 (1997) 1–22.